Supporting Information

Ultra-broad Bandwidth and Highly Sensitive Optical Ultrasonic Detector for Photoacoustic Imaging

*Cheng Zhang, Tao Ling, Sung-Liang Chen and L. Jay Guo**

Department of Electrical Engineering and Computer Science, University of Michigan, Ann Arbor, MI, USA 48109

Email: guo@umich.edu

Supporting information includes: Device fabrication; Bandwidth calculation; Detector frequency response extrapolation; Bandwidth simulation; There are two figures and 5 pages. This information is available free of charge via the Internet at http://pubs.acs.org/photonics.

Device fabrication: The silicon mold was fabricated by electron beam lithography (E-beam) to define the microring and the bus waveguide pattern at first. The E-beam resist was polymethyl methacrylate (PMMA). After resist development, a thermal reflow process (115℃, 90s) was applied to reduce imperfections in PMMA and harden its edge. Then the PMMA was used as the mask in plasma coupled reactive ion etching (RIE) to transfer the pattern onto silicon. At last, the PMMA was removed by acetone which concludes the mold fabrication process[1]. Then the silicon mold was employed in a thermal imprinting process on polystyrene (PS) film (Nanonex 2000).

Bandwidth calculation: The measured photoacoustic signal by the microring detector in the frequency domain can be expressed as follows:

$$F_{signal} = F_{laser} \times F_{water} \times F_{ring} \times F_{\det ector}$$

In which, F_{signal} is the detected photoacoustic signal, F_{laser} is the laser signal, F_{water} is the water frequency-dependent transfer function and represents different attenuations for different frequency components. F_{ring} is the microring frequency response, and $F_{\det ector}$ is the photo detector response. All the parameters are in the frequency domain.

The microring frequency response can be calculated by:

$$F_{ring} = \frac{F_{signal}}{F_{laser} \times F_{\det ector} \times F_{water}}$$

A 20-μm propagation distance in water, which is the gap between the Cr film and the microring in experiment, was used in the calculation of F_{water}. By measuring the laser signal with the same photo detector, $F_{laser} \times F_{\det ector}$ as a whole can be determined.

Detector frequency response extrapolation: Due to the limited laser pulse width and photo detector bandwidth/sensitivity, the microring response at -6 dB cannot be directly characterized. A Gaussian function is used to extrapolate the ring response spectrum, shown in figure SI 1. The ring is expected to have a -6 dB bandwidth at 470 MHz. This leads to a detector FWHM bandwidth of 940 MHz. Applying the formula R = 0.88C/BW gives an axial resolution of 1.4 μm, which is in agreement with the result from the "shift and sum" method.

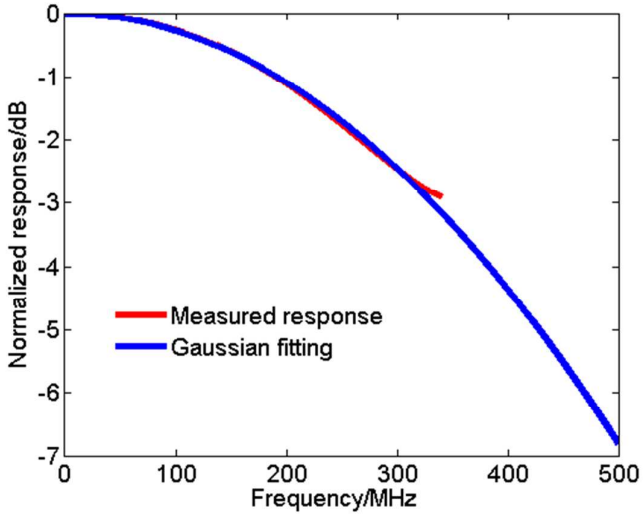

Figure SI 1: Ring response spectrum and its Gaussian functional extrapolation, showing the detector -6 dB response at 470 MHz, and the detector FWHM bandwidth is 940 MHz.

Bandwidth simulation: An ultrasound wave with certain frequency will bounce back and forth in the acoustic cavity formed by PS/water and PS/SiO2 boundaries under the plane wave approximation. This leads to an acoustic wave amplitude distribution in the PS waveguide region along the vertical direction. Such distribution is integrated over the whole waveguide core area to have an effective in modulating the waveguide property and the ring resonance behavior[2].

In the above analysis, the optical field profile inside the PS waveguide has an important effect.

Since the optical field is more concentrated in the waveguide central area, an acoustic wave with enhanced amplitude in the central regime of the waveguide will have a larger effect on changing ring behavior than a wave concentrated in edge regime of the waveguide. In other words, optical field distribution acts as a "weighting factor" in analyzing the device acoustic frequency response. However, how the optical field distribution would affect the device acoustic response is a complex problem by itself. In this estimation, we use the optical field distribution in the vertical direction of the waveguide center as the "weighting factor" and this is in line with our plane wave approximation.

Figure SI 2a shows the optical field distribution for TE mode, as in the case of the experiment (TM has similar results). Figure SI 2b shows the simulated and the measured frequency response spectra. The simulated response has a -3dB response at 315 MHz and the measured one has -3dB at 350 MHz. And there are differences in their curve shapes. The discrepancy can be attributed to factors such as the plane wave approximation we used, how the optical filed distribution is taken into account, as well as material parameters used in simulation. Further investigation is currently underway.

The acoustic impedances used in the acoustic bandwidth simulation for water, PS and SiO_2 are 1.49×10^6 Kg/(s•m^2), 2.47×10^6 Kg/(s•m^2) and 1.31×10^7 Kg/(s•m^2)^3, respectively. For the optical field profile calculation, the refractive indices for water, PS and SiO_2 are 1.33, 1.578 and 1.46 respectively[4].

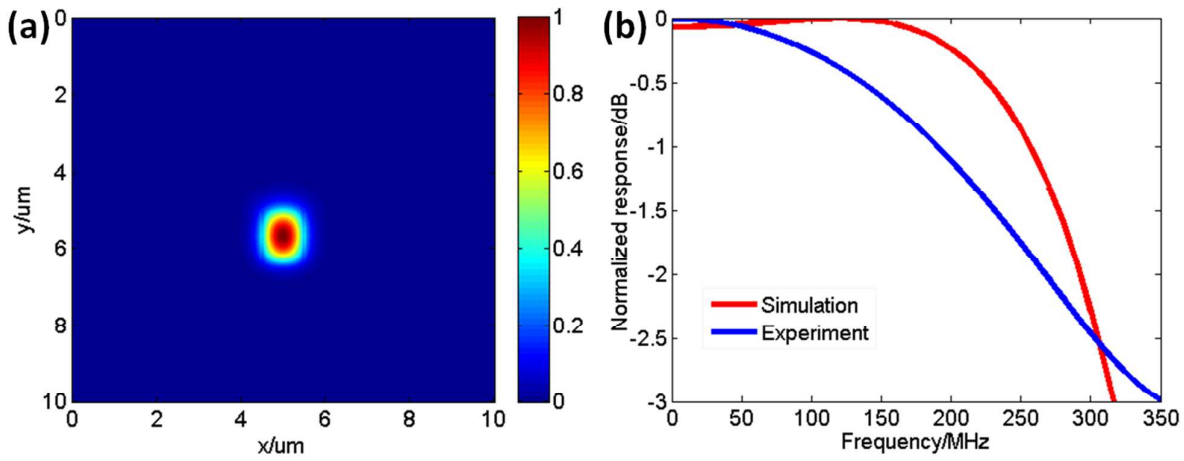

Figure SI 2: (a) Simulated transverse electric (TE) mode distribution; (b) Comparison of simulated and measured frequency response.

1. Ling, T.; Chen, S.-L.; Guo, L. J., High-sensitivity and wide-directivity ultrasound detection using high Q polymer microring resonators. *Appl. Phys. Lett.* **2011,** *98*, 204103

2. Beard, P. C.; Perennes, F.; Mills, T. N., Transduction mechanisms of the Fabry-Perot polymer film sensing concept for wideband ultrasound detection. *IEEE Trans. Ultrason. Ferroelectr. Freq. Control,* **1999,** *46*, 1575-1582.

3. Sinha, M.; Buckley, D., Acoustic Properties of Polymers. In *Physical Properties of Polymers Handbook*, Mark, J., Ed. Springer New York: 2007, 1021-1031.

4. Brandrup, J.; Immergut, E. H.; Grulke, E. A.; Abe, A.; Bloch, D. R., Polymer Handbook (4th Edition). John Wiley & Sons.